J. Phys. D: Appl. Phys. **33** (2000) 1697–1704. Printed in the UK PII: S0022-3727(00)13375-3

UV OH spectrum used as a molecular pyrometer

Charles de Izarra

Faculté des Sciences, Site de Bourges, Université d'Orléans, rue Gaston Berger, BP 4043, 18028 Bourges Cedex, France

Received 19 April 2000

Abstract. For the UV OH band at 306.357 nm (transition $A^2\Sigma$, $v = 0 \rightarrow X^2\Pi$, $v' = 0$) that is frequently observed in hot gases containing oxygen and hydrogen (flames, arc plasmas), a very sensitive variation of two groups of unresolved rotational lines as a function of the temperature has been found. Using a numerical simulation, this variation has been calibrated as a function of the temperature and of the optical apparatus function. This calibration allows us to easily determine the rotational temperature without computing any line intensity.

1. Introduction

Molecular spectra [1] can successfully give information in the temperature range 2000–8000 K where atomic spectra are not strong enough to ensure a good sensitivity [2]. To determine the rotational temperature of a diatomic gas, that is generally close to its heavy species kinetic temperature, a possible method is the well known Boltzmann plot, assuming a rather high resolution optical device is available to resolve rotational lines. On the other hand—and it is most frequently the case with *in situ* industrial studies—molecular spectra are recorded with a poor spectral resolution that does not allow the observation of the resolved rotational lines. In this case, it is useful to compare experimental data with a computed synthetic spectrum that takes into account both the temperature and the optical apparatus function effects [3]. However, the comparison of experimental data with a synthetic molecular spectrum is often difficult to perform and previous published works do not give precise details of the fitting procedure employed. In addition, to determine the temperature, most authors deal with intensities of unresolved groups of rotational lines supposing the definition of a given spectral range. In this work, from a numerical simulation of the UV OH spectrum and an original normalization of the synthetic spectra, it has been possible to produce a calibration of the maximum amplitude of two groups of unresolved rotational lines, which are very sensitive, as a function of the temperature.

2. The UV OH spectrum

2.1. Generalities

The intensity I_{nm} of a spectral line corresponding to a transition $(n \rightarrow m)$ between two levels is given by

$$I_{nm} = N_n A_{nm} h \nu_{nm} \tag{1}$$

where h is Planck's constant, ν_{nm} the frequency of the transition, A_{nm} the spontaneous transition probability and N_n the particle density in the initial state $|n\rangle$. A simple thermodynamics model commonly employed, giving N_n as a function of the temperature T, may be found, assuming thermodynamics equilibrium and Boltzmann's law

$$N_n = \frac{N_0 g_n}{Z(T)} \exp\left(-\frac{E_n}{kT}\right) \tag{2}$$

where k is the Boltzmann constant, N_0 the particle density, $Z(T)$ the partition function of the particle, g_n and E_n the statistical weight and the energy of the state $|n\rangle$, respectively. From equations (1) and (2), another expression of I_{nm} is

$$I_{nm} = \frac{K_{nm}}{Z(T)} \exp\left(-\frac{E_n}{kT}\right) \tag{3}$$

where $K_{nm} = N_0 A_{nm} g_n h \nu_{nm}$ is a constant for a given transition $(n \rightarrow m)$.

In the case when I_{nm} is known for a given temperature T_{ref} ($I_{nm_{\mathrm{ref}}}$ is taken for reference), we can write:

$$I_{nm} = I_{nm_{\mathrm{ref}}} \frac{Z(T_{\mathrm{ref}})}{Z(T)} \exp\left(-\frac{E_n(T_{\mathrm{ref}} - T)}{T_{\mathrm{ref}} T}\right). \tag{4}$$

At least, it is important to emphasize that the general procedure of temperature measurements from molecular band spectra does not need to consider absolute values of light intensities. Since, most of the time, experimental data are relative values, we can consider only theoretical relative values, as given in equation (4).

2.2. The UV OH spectrum

The OH UV spectrum is frequently observed in many kinds of flames and hot gases containing oxygen and hydrogen. In addition, the rotational temperature of the OH radical is close to the gas temperature [3], i.e. to the temperature

0022-3727/00/141697+08$30.00

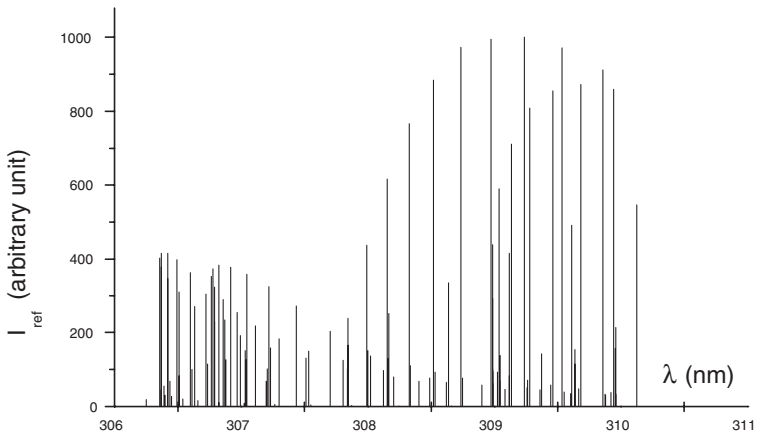

Figure 1. Plot of the rotational lines of OH spectrum represented as Dirac impulses for the reference temperature $T_{\text{ref}} = 3000$ K. Reference data are from the paper by Diecke and Crosswhite [4].

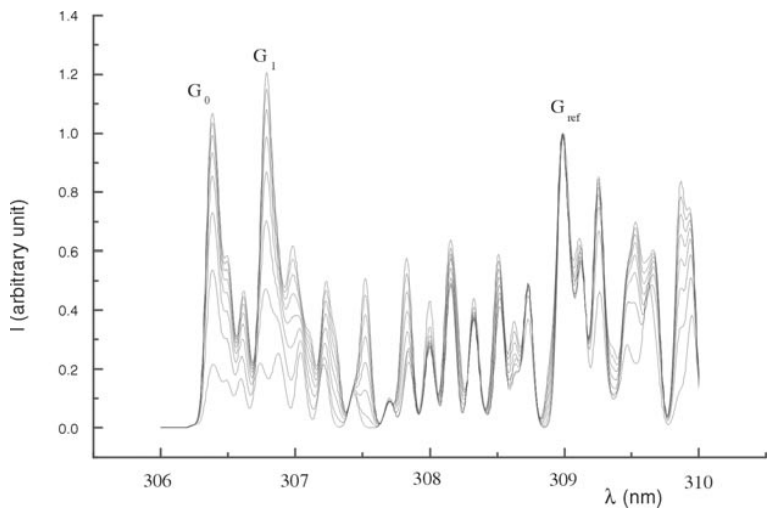

Figure 2. Plot of the UV OH spectrum for the rotational temperature varying from 1000–8000 K, in 1000 K steps ($\Delta = 0.1$ nm).

determined using an enthalpy balance. The OH band ($A^2\Sigma$, $\nu = 0 \rightarrow X^2\Pi$, $\nu' = 0$) has been studied thoroughly by Dieke and Crosswhite [4], and shows a red degradation with four main band heads R_1, R_2, Q_1, Q_2 at 306.537 nm, 306.776 nm, 307.844 nm and 308.986 nm, respectively. The paper by Diecke and Crosswhite [4] gives the wavelengths of the different rotational lines of the different branches, the energy of the upper level of each transition (in cm^{-1}), and the normalized intensity $I_{nm_{\text{ref}}}$ of each line for a reference temperature $T_{\text{ref}} = 3000$ K.

Figure 1 gives a plot of the rotational lines represented as Dirac impulses for the reference temperature $T_{\text{ref}} = 3000$ K. Rotational lines are presented in table 1, and the corresponding data are used as input data in the simulation program. We have to emphasize that some weak transitions are given in [4] without being attributed to any coherent transition of the OH spectrum. Consequently, these weak transitions have been omitted in our procedure.

2.3. Optical apparatus function

In experimental spectroscopy, it is necessary to measure the apparatus function either by employing a laser line (that may be considered as a Dirac impulse $\delta(\lambda_0)$) or by employing sharp lines emitted by a spectral lamp (a low pressure mercury lamp for example). In many experimental conditions, the apparatus function (i.e. the impulse response of the optical device) can be well fitted with a Gaussian profile as a function of the wavelength λ. In addition, lines emitted by hot gases are broadened by different effects [3]. Consequently, the best way to mathematically represent the apparatus function is to consider a normalized Gaussian profile given by:

$$G(\lambda) = \frac{2}{\Delta\sqrt{\pi}} \exp\left(-\frac{(\lambda - \lambda_0)^2}{(\Delta/2)^2}\right) \tag{5}$$

where Δ represents the full width at 1/e of the maximum located at the wavelength λ_0.

3. Numerical simulation: calibration

Using reference data and equation (4), a Dirac synthetic spectrum is first computed for a given temperature T, assuming that $Z(T_{\text{ref}})/Z(T) = 1$ in equation (4). Then, the Dirac spectrum is convoluted with a Gaussian apparatus function (equation (5)) to produce a synthetic spectrum.

Table 1. Parameters of the rotational lines used to proceed to numerical simulation of the UV OH molecular band. Reference data are from the paper by Diecke and Crosswhite [4].

λ (nm)	I_{ref} (3000 K)	E_u (cm^{-1})	λ (nm)	I_{ref} (3000 K)	E_u (cm^{-1})	λ (nm)	I_{ref} (3000 K)	E_u (cm^{-1})
306.2523	19	32 643.45	307.2009	69	32 542.56	308.9861	62	33 383.26
306.3565	402	34 282.99	307.2063	102	32 541.98	308.9861	293	32 541.98
306.3725	415	33 951.80	307.2199	325	33 148.73	308.9861	95	32 542.56
306.3725	378	34 645.53	307.2308	159	37 443.91	308.9861	439	32 643.45
306.3725	44	34 280.64	307.2660	6	37 440.15	308.9861	100	32 644.22
306.3921	55	33 949.67	307.3028	183	36 902.90	309.0270	94	32 779.49
306.3970	31	34 642.92	307.4369	273	32 947.05	309.0364	589	32 778.49
306.4189	415	33 652.29	307.5123	131	38 007.90	309.0449	70	32 474.62
306.4236	346	35 038.61	307.5334	151	37 440.15	309.0473	139	32 474.30
306.4370	68	33 650.38	307.5486	5	38 003.93	309.0862	47	40 513.79
306.4491	27	35 035.86	307.7028	204	32 778.49	309.1186	416	32 542.56
306.4950	397	33 384.97	307.8071	125	38 003.93	309.1186	83	32 948.31
306.5095	310	35 462.01	307.8373	102	38 597.79	309.1361	712	32 947.05
306.5095	83	33 383.26	307.8440	239	32 474.62	309.2394	1000	33 652.29
306.5372	20	35 459.02	307.8468	166	32 474.30	309.2577	50	33 650.38
306.5976	363	33 150.14	307.8753	3	38 003.93	309.2650	71	33 148.73
306.6114	100	33 148.73	307.9951	437	32 542.56	309.2786	808	33 148.73
306.6318	271	35 914.82	308.0006	152	32 541.98	309.3609	45	40 513.79
306.6613	15	35 911.59	308.0231	138	32 643.45	309.3722	143	32 440.61
306.7240	304	32 948.31	308.1255	98	38 593.62	309.4459	58	33 150.14
306.7356	114	32 947.05	308.1541	616	32 644.22	309.4618	855	33 383.26
306.7661	352	34 642.92	308.1620	130	32 643.45	309.5342	973	33 951.80
306.7775	373	34 280.64	308.1665	252	32 440.61	309.5546	40	33 949.67
306.7929	230	36 396.66	308.2065	80	39 212.69	309.6000	35	41 198.19
306.7929	323	35 035.86	308.2456	2	39 208.99	309.6124	492	32 644.22
306.8277	11	36 393.24	308.3278	766	32 779.49	309.6349	114	32 474.30
306.8277	383	33 949.67	308.3374	111	32 778.49	309.6349	154	32 474.62
306.8608	290	35 459.02	308.4050	68	32 541.98	309.6650	48	33 384.97
306.8704	234	32 779.49	308.4894	77	39 208.99	309.6830	873	33 650.38
306.8799	126	32 778.49	308.5196	884	32 948.31	309.8586	912	34 282.99
306.9177	378	33 650.38	308.5317	93	32 947.05	309.8715	34	41 193.51
306.9675	255	35 911.59	308.6226	66	39 851.66	309.8807	31	34 280.64
306.9913	193	36 906.50	308.6390	335	32 474.62	309.9210	38	33 949.67
307.0244	9	36 902.90	308.6634	2	39 847.20	309.9411	860	33 949.67
307.0318	152	32 644.22	308.7338	974	33 150.14	309.9538	158	32 644.22
307.0392	127	32 643.45	308.7481	77	33 148.73	309.9593	215	32 541.98
307.0478	359	33 383.26	308.9008	59	39 847.20	309.9593	33	32 440.61
307.1145	218	36 393.24	308.9734	995	33 384.97			

A set of about 2000 synthetic spectra has been computed for temperatures varying from 600–9000 K, in 200 K steps, and for Δ varying from 0.02–0.98 nm, in 0.02 nm steps. This data set is stored on disc for data processing.

Figure 2 gives a plot of synthetic spectra for an apparatus function width $\Delta = 0.1$ nm and for a rotational temperature varying from 1000–8000 K, in 1000 K steps. An important point is that all the synthetic spectra have been normalized against the intensity of the group of unresolved rotational lines G_{ref} (see figure 2) at ≈309 nm, which appears to be the relative strongest group of unresolved lines when the rotational temperature is lower than 4000 K.

A quick survey of figure 2 shows the presence of two groups of unresolved rotational lines, G_0 and G_1, the amplitudes of which are very sensitive against the rotational temperature. A more detailed analysis of the groups G_0 and G_1 shows that the wavelength of their maximum amplitude varies as a function of the temperature T.

In order to avoid the difficulties encountered in experimental measurements of group line intensities it has been decided to only consider the maximum amplitude of the groups of lines G_0 and G_1 as a function of the temperature. It is obvious that this choice is dependent on the apparatus function width Δ that must be precisely determined.

The typical evolution of the maximum amplitude of G_0/G_{ref} and G_1/G_{ref} as a function of the rotational temperature is given in figure 3 for an apparatus function width $\Delta = 0.12$ nm. From figure 3, we notice a high sensitivity of these maxima in the temperature range 1000–4000 K. This sensitivity decreases when the temperature is higher than 4000 K, and then leads to an increase of the error percentage in a temperature determination.

For a practical determination of the temperature from an experimental UV OH spectrum recorded with a known apparatus function width, we give the tables 2, 3, 4 and 5 that present the ratios G_0/G_{ref} and G_1/G_{ref} for different values of temperature T and apparatus function width Δ.

4. Check of the method

4.1. Published works

A check of the temperature determination method has been made by considering the OH spectra given in [3]. The authors

Table 2. Maximum amplitude of the unresolved group of rotational lines G_0 as a function of the temperature and for Δ varying from 0.04–0.2 nm.

T (K)	0.04 nm	0.06 nm	0.08 nm	0.10 nm	0.12 nm	0.14 nm	0.16 nm	0.18 nm	0.2 nm
600	0.046 33	0.053 45	0.065 17	0.068 99	0.071 94	0.074 98	0.077 57	0.080 10	0.082 10
800	0.106 40	0.115 40	0.130 77	0.139 35	0.144 54	0.149 19	0.152 63	0.155 13	0.156 62
1000	0.173 40	0.186 27	0.204 51	0.216 03	0.222 53	0.228 82	0.232 98	0.235 27	0.236 02
1200	0.239 13	0.255 09	0.276 76	0.291 54	0.299 18	0.306 36	0.311 45	0.313 62	0.313 60
1400	0.300 16	0.318 76	0.344 32	0.362 39	0.371 44	0.378 93	0.384 83	0.387 07	0.386 51
1600	0.355 49	0.376 35	0.405 65	0.426 49	0.437 29	0.445 73	0.452 18	0.454 61	0.453 44
1800	0.405 17	0.427 98	0.460 83	0.484 39	0.496 76	0.506 12	0.513 28	0.515 84	0.514 34
2000	0.449 64	0.474 15	0.510 35	0.536 53	0.550 40	0.560 64	0.568 27	0.571 14	0.569 42
2200	0.489 47	0.515 48	0.554 82	0.583 55	0.598 76	0.609 78	0.617 83	0.620 98	0.619 06
2400	0.525 23	0.552 56	0.594 82	0.626 02	0.642 38	0.654 07	0.662 47	0.665 82	0.663 60
2600	0.557 42	0.585 94	0.630 92	0.664 41	0.681 83	0.694 03	0.702 67	0.706 14	0.703 56
2800	0.586 52	0.616 09	0.663 59	0.699 19	0.717 60	0.730 15	0.738 91	0.742 39	0.739 42
3000	0.612 89	0.643 43	0.693 28	0.730 81	0.750 06	0.762 84	0.771 62	0.774 93	0.771 60
3200	0.636 06	0.668 31	0.720 08	0.759 63	0.779 60	0.792 48	0.801 17	0.804 15	0.800 48
3400	0.657 20	0.691 04	0.744 51	0.785 99	0.806 55	0.819 25	0.827 91	0.830 46	0.826 41
3600	0.676 56	0.711 86	0.766 90	0.810 17	0.831 00	0.843 63	0.852 15	0.854 18	0.849 69
3800	0.694 34	0.731 01	0.787 51	0.832 22	0.853 39	0.865 87	0.874 15	0.875 57	0.870 62
4000	0.710 72	0.748 66	0.806 51	0.852 49	0.873 96	0.886 21	0.894 06	0.894 90	0.889 44
4200	0.725 87	0.764 99	0.824 10	0.871 22	0.892 91	0.904 84	0.912 19	0.912 39	0.906 38
4400	0.739 90	0.780 14	0.840 41	0.888 57	0.910 41	0.921 95	0.928 73	0.928 22	0.921 64
4600	0.752 94	0.794 21	0.855 57	0.904 69	0.926 59	0.937 69	0.943 84	0.942 57	0.935 40
4800	0.765 08	0.807 34	0.869 71	0.919 69	0.941 59	0.952 19	0.957 67	0.955 59	0.947 81
5000	0.776 42	0.819 59	0.882 92	0.933 68	0.955 53	0.965 59	0.970 35	0.967 43	0.959 03
5200	0.787 03	0.831 07	0.895 28	0.946 76	0.968 51	0.977 98	0.981 99	0.978 20	0.969 17
5400	0.796 98	0.841 83	0.906 87	0.959 01	0.980 61	0.989 46	0.992 70	0.988 02	0.978 34
5600	0.806 32	0.851 94	0.917 77	0.970 50	0.991 92	1.000 11	1.002 56	0.996 97	0.986 65
5800	0.815 12	0.861 46	0.928 03	0.981 30	1.002 49	1.010 02	1.011 66	1.005 14	0.994 17
6000	0.823 41	0.870 44	0.937 70	0.991 46	1.012 41	1.019 25	1.020 06	1.012 62	1.001 00
6200	0.831 24	0.878 92	0.946 83	1.001 05	1.021 72	1.027 85	1.027 83	1.019 46	1.007 20
6400	0.838 65	0.886 95	0.955 47	1.010 10	1.030 48	1.035 89	1.035 03	1.025 73	1.012 84
6600	0.845 66	0.894 55	0.963 66	1.018 66	1.038 72	1.043 40	1.041 71	1.031 48	1.017 96
6800	0.852 31	0.901 76	0.971 42	1.026 77	1.046 49	1.050 44	1.047 91	1.036 75	1.022 61
7000	0.858 63	0.908 62	0.978 80	1.034 45	1.053 83	1.057 05	1.053 68	1.041 60	1.026 85
7200	0.864 64	0.915 13	0.985 81	1.041 75	1.060 77	1.063 25	1.059 04	1.046 07	1.030 71
7400	0.870 36	0.921 25	0.992 48	1.048 69	1.067 34	1.069 08	1.064 05	1.050 17	1.034 22
7600	0.875 81	0.927 06	0.998 85	1.055 29	1.073 56	1.074 57	1.068 72	1.053 96	1.037 43
7800	0.881 02	0.932 61	1.004 92	1.061 58	1.079 47	1.079 74	1.073 08	1.057 45	1.040 35
8000	0.885 99	0.937 92	1.010 72	1.067 57	1.085 08	1.084 62	1.077 16	1.060 67	1.043 01

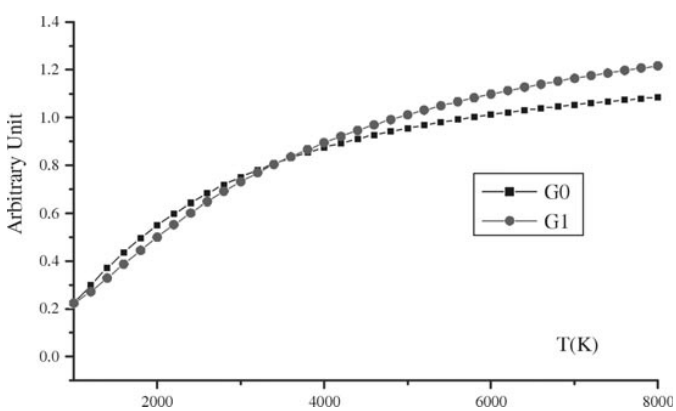

Figure 3. Plot of the maxima amplitudes of the groups of unresolved lines as a function of the temperature for the apparatus function width $\Delta = 0.12$ nm.

give the apparatus function by considering the full width at half maximum (FWHM) δ of a Gaussian profile. For comparison, the δ parameter has been transformed into the full width at 1/e of the maximum with the relation $\delta = \Delta\sqrt{\ln 2}$. In all cases, since the spectra have been recorded in plasmas with copper electrodes, only the group of unresolved lines G_1 has been considered, because of the presence of a copper line at the wavelength $\lambda = 306.341$ nm that can perturbate the amplitude of the group G_0. Pellerin *et al* [3] presented a figure of the UV OH spectrum recorded on a plasma jet containing water. The spectrum was obtained with an optical apparatus function width $\Delta = 0.0456$ nm. Using a rule, it is easy to measure the amplitudes of the unresolved groups of rotational lines G_1 and G_{ref}. Graphical

Table 3. Maximum amplitude of the unresolved group of rotational lines G_0 as a function of the temperature and for Δ varying from 0.22–0.38 nm.

T (K)	0.22 nm	0.24 nm	0.26 nm	0.28 nm	0.30 nm	0.32 nm	0.34 nm	0.36 nm	0.38 nm
600	0.084 24	0.086 60	0.089 12	0.091 75	0.094 46	0.097 20	0.100 50	0.103 26	0.106 02
800	0.158 18	0.159 94	0.161 87	0.163 90	0.165 98	0.168 10	0.170 68	0.172 85	0.175 04
1000	0.236 54	0.237 16	0.237 90	0.238 70	0.239 52	0.240 37	0.241 49	0.242 51	0.243 64
1200	0.313 09	0.312 41	0.311 73	0.311 04	0.310 29	0.309 61	0.308 98	0.308 64	0.308 53
1400	0.384 91	0.383 05	0.380 93	0.378 68	0.376 32	0.374 06	0.371 56	0.369 81	0.368 42
1600	0.451 04	0.448 05	0.444 57	0.440 83	0.436 90	0.433 03	0.428 75	0.425 62	0.423 00
1800	0.511 26	0.507 19	0.502 50	0.497 35	0.491 94	0.486 54	0.480 53	0.476 12	0.472 35
2000	0.565 68	0.560 69	0.554 89	0.548 44	0.541 64	0.534 85	0.527 23	0.521 60	0.516 74
2200	0.614 65	0.608 89	0.602 08	0.594 44	0.586 35	0.578 27	0.569 18	0.562 44	0.556 62
2400	0.658 68	0.652 20	0.644 48	0.635 76	0.626 48	0.617 21	0.606 77	0.599 04	0.592 29
2600	0.698 18	0.691 05	0.682 49	0.672 78	0.662 45	0.652 09	0.640 43	0.631 76	0.624 23
2800	0.733 60	0.725 86	0.716 52	0.705 92	0.694 62	0.683 30	0.670 53	0.661 02	0.652 76
3000	0.765 34	0.757 01	0.746 96	0.735 56	0.723 39	0.711 19	0.697 40	0.687 17	0.678 23
3200	0.793 76	0.784 88	0.774 18	0.762 04	0.749 09	0.736 11	0.721 41	0.710 50	0.700 98
3400	0.819 23	0.809 78	0.798 48	0.785 69	0.772 05	0.758 36	0.742 84	0.731 33	0.721 30
3600	0.842 04	0.832 03	0.820 19	0.806 82	0.792 54	0.778 23	0.761 99	0.749 93	0.739 43
3800	0.862 48	0.851 94	0.839 58	0.825 68	0.810 84	0.795 96	0.779 08	0.766 55	0.755 61
4000	0.880 80	0.869 74	0.856 90	0.842 52	0.827 17	0.811 80	0.794 36	0.781 39	0.770 06
4200	0.897 21	0.885 68	0.872 39	0.857 56	0.841 76	0.825 94	0.808 00	0.794 65	0.782 98
4400	0.911 93	0.899 95	0.886 23	0.871 00	0.854 79	0.838 58	0.820 19	0.806 51	0.794 53
4600	0.925 15	0.912 72	0.898 60	0.883 01	0.866 44	0.849 87	0.831 10	0.817 11	0.804 86
4800	0.937 04	0.924 17	0.909 67	0.893 74	0.876 84	0.859 97	0.840 85	0.826 59	0.814 10
5000	0.947 73	0.934 43	0.919 57	0.903 33	0.886 14	0.869 01	0.849 57	0.835 08	0.822 37
5200	0.957 34	0.943 63	0.928 43	0.911 91	0.894 46	0.877 08	0.857 38	0.842 68	0.829 78
5400	0.966 00	0.951 89	0.936 36	0.919 57	0.901 89	0.884 31	0.864 36	0.849 48	0.836 41
5600	0.973 80	0.959 30	0.943 46	0.926 43	0.908 54	0.890 77	0.870 62	0.855 58	0.842 35
5800	0.980 84	0.965 95	0.949 82	0.932 56	0.914 49	0.896 55	0.876 22	0.861 04	0.847 68
6000	0.987 18	0.971 92	0.955 52	0.938 04	0.919 82	0.901 73	0.881 24	0.865 93	0.852 45
6200	0.992 90	0.977 28	0.960 62	0.942 94	0.924 57	0.906 36	0.885 74	0.870 31	0.856 73
6400	0.998 07	0.982 10	0.965 18	0.947 33	0.928 83	0.910 50	0.889 76	0.874 24	0.860 56
6600	1.002 74	0.986 42	0.969 27	0.951 25	0.932 63	0.914 20	0.893 36	0.877 76	0.863 99
6800	1.006 95	0.990 31	0.972 93	0.954 75	0.936 03	0.917 51	0.896 59	0.880 91	0.867 07
7000	1.010 75	0.993 79	0.976 20	0.957 87	0.939 06	0.920 47	0.899 47	0.883 72	0.869 82
7200	1.014 19	0.996 92	0.979 12	0.960 66	0.941 77	0.923 10	0.902 05	0.886 24	0.872 29
7400	1.017 27	0.999 73	0.981 73	0.963 14	0.944 17	0.925 46	0.904 35	0.888 50	0.874 49
7600	1.020 06	1.002 24	0.984 05	0.965 34	0.946 32	0.927 55	0.906 40	0.890 51	0.876 46
7800	1.022 57	1.004 49	0.986 12	0.967 30	0.948 22	0.929 41	0.908 22	0.892 30	0.878 21
8000	1.024 83	1.006 50	0.987 96	0.969 04	0.949 91	0.931 06	0.909 85	0.893 89	0.879 78

measurement gives $G_1 = 30$ mm and $G_{\text{ref}} = 41$ mm, leading to a ratio (without unity) $G_1/G_{\text{ref}} = 0.73$. With a linear interpolation in table 4 to obtain data corresponding to $\Delta = 0.0456$ nm, we find a temperature value of 4000 K. This value is in close agreement with the temperature value of 4100 K proposed by the authors.

4.2. Recombining plume of an argon plasma jet

It is now well established that dc argon plasma jets can have two kinds of flows, depending on the values of the plasma gas flow rate [5], on the current intensity and on the anode nozzle diameter. In the case of a turbulent flow, the plasma jet is short and very noisy. On the other hand, in a laminar flow, the jet is well structured with a hot and bright core followed by a recombining plume, the length of which can reach about ten centimetres. The axial temperature profile shows a rapid decrease as a function of the distance from the anode.

In the laminar recombining plume, the temperature is generally too low to employ emission atomic spectroscopy (including line intensity ratio or line broadening) and, consequently, other methods have been used in the past, such as *in situ* probes, or interferometry [6, 7].

The temperature determination presented here is realized in the plume of a laminar argon plasma jet.

4.2.1. Experimental set-up. The experimental set-up includes a commercial dc plasma torch (SAF Soudure Autogène Française trademark) operating at atmospheric pressure in ambient air, with an axial injection of pure argon controlled with flowmeters. The arc current intensity, limited at 250 A is supplied by an ac/dc power converter (Soudure Autogène Française trademark). The anode is in copper, and the cathode is in tungsten; the electrodes are water cooled.

The experimental conditions presented in this paper have been chosen to produce an argon laminar jet. The experimental conditions are as follows: for an anode diameter of 3 mm, the gas flow rate is 6 slm and the current intensity is 120 A.

The spectroscopic acquisition chain includes a Cromex monochromator of the Ébert–Fastié type, with a focal length of 0.5 m. It has a 1200 grooves mm^{-1} grating working in the first order. Photodetection is accomplished with a Princeton OMA III equipped with a matrix CCD array having 512 rows of 1024 pixels. In the first spectroscopic order, the detector covers a spectral range of 45 nm. A CaF_2 lens (transparent

Table 4. Maximum amplitude of the unresolved group of rotational lines G_1 as a function of the temperature and for Δ varying from 0.04–0.2 nm.

T (K)	0.04 nm	0.06 nm	0.08 nm	0.10 nm	0.12 nm	0.14 nm	0.16 nm	0.18 nm	0.2 nm
600	0.074 20	0.121 48	0.138 11	0.139 03	0.138 62	0.140 16	0.151 66	0.166 30	0.175 24
800	0.088 79	0.149 45	0.173 60	0.178 80	0.180 88	0.184 44	0.202 14	0.218 89	0.228 75
1000	0.103 16	0.174 37	0.207 96	0.218 18	0.223 88	0.236 46	0.258 55	0.276 72	0.287 08
1200	0.155 32	0.197 71	0.241 16	0.258 19	0.272 09	0.293 94	0.317 94	0.337 23	0.347 83
1400	0.208 82	0.237 99	0.277 87	0.306 72	0.328 78	0.353 43	0.377 92	0.398 12	0.408 93
1600	0.261 46	0.295 22	0.332 75	0.362 30	0.388 04	0.414 59	0.438 35	0.458 38	0.468 84
1800	0.312 09	0.350 33	0.388 93	0.418 62	0.445 87	0.473 19	0.496 83	0.516 27	0.526 56
2000	0.360 15	0.402 73	0.442 89	0.473 10	0.501 12	0.528 79	0.552 13	0.571 30	0.581 27
2200	0.405 42	0.452 73	0.494 54	0.524 83	0.553 18	0.581 14	0.604 13	0.622 97	0.632 62
2400	0.448 99	0.500 21	0.543 33	0.573 40	0.602 20	0.630 17	0.652 79	0.671 18	0.680 46
2600	0.490 57	0.544 77	0.589 07	0.619 17	0.648 15	0.675 93	0.698 16	0.715 97	0.724 83
2800	0.529 61	0.586 54	0.631 90	0.662 20	0.691 06	0.718 56	0.740 28	0.757 46	0.765 83
3000	0.566 24	0.625 67	0.672 00	0.702 44	0.731 10	0.758 22	0.779 35	0.795 79	0.803 63
3200	0.599 82	0.662 34	0.709 30	0.740 09	0.768 48	0.795 08	0.815 53	0.831 08	0.838 41
3400	0.631 32	0.696 73	0.744 15	0.775 32	0.803 36	0.829 19	0.849 03	0.863 61	0.870 37
3600	0.660 88	0.728 99	0.776 82	0.808 33	0.835 75	0.860 92	0.880 06	0.893 59	0.899 73
3800	0.688 65	0.759 30	0.807 47	0.839 08	0.865 99	0.890 44	0.908 79	0.921 20	0.926 69
4000	0.714 77	0.787 81	0.836 28	0.867 87	0.894 29	0.917 94	0.935 33	0.946 65	0.951 44
4200	0.739 36	0.814 65	0.863 37	0.894 92	0.920 79	0.943 58	0.959 93	0.970 12	0.974 17
4400	0.762 55	0.839 95	0.889 03	0.920 36	0.945 63	0.967 50	0.982 76	0.991 76	0.995 04
4600	0.784 44	0.863 83	0.913 36	0.944 31	0.968 95	0.989 85	1.003 98	1.011 75	1.014 24
4800	0.805 13	0.886 40	0.936 34	0.966 91	0.990 87	1.010 76	1.023 71	1.030 21	1.031 89
5000	0.824 71	0.907 76	0.958 07	0.988 24	1.011 50	1.030 33	1.042 09	1.047 29	1.048 14
5200	0.843 26	0.927 99	0.978 65	1.008 40	1.030 93	1.048 68	1.059 21	1.063 10	1.063 11
5400	0.860 86	0.947 19	0.998 16	1.027 49	1.049 26	1.065 90	1.075 19	1.077 75	1.076 91
5600	0.877 58	0.965 42	1.016 68	1.045 57	1.066 58	1.082 09	1.090 12	1.091 34	1.089 66
5800	0.893 47	0.982 75	1.034 27	1.062 73	1.082 95	1.097 32	1.104 09	1.103 96	1.101 43
6000	0.908 59	0.999 24	1.051 01	1.079 02	1.098 45	1.111 66	1.117 17	1.115 70	1.112 32
6200	0.923 01	1.014 96	1.066 96	1.094 51	1.113 13	1.125 19	1.129 43	1.126 62	1.122 40
6400	0.936 75	1.029 95	1.082 15	1.109 26	1.127 07	1.137 96	1.140 94	1.136 80	1.131 74
6600	0.949 88	1.044 26	1.096 66	1.123 31	1.140 30	1.150 03	1.151 75	1.146 29	1.140 41
6800	0.962 42	1.057 94	1.110 51	1.136 71	1.152 89	1.161 45	1.161 92	1.155 15	1.148 46
7000	0.974 42	1.071 02	1.123 75	1.149 51	1.164 86	1.172 27	1.171 50	1.163 44	1.155 94
7200	0.985 91	1.083 54	1.136 43	1.161 73	1.176 27	1.182 53	1.180 53	1.171 19	1.162 90
7400	0.996 92	1.095 43	1.148 57	1.173 42	1.187 15	1.192 26	1.189 05	1.178 46	1.169 38
7600	1.007 48	1.106 81	1.160 20	1.184 61	1.197 53	1.201 51	1.197 10	1.185 27	1.175 42
7800	1.017 61	1.117 74	1.171 37	1.195 34	1.207 44	1.210 30	1.204 71	1.191 66	1.181 06
8000	1.027 34	1.128 24	1.182 09	1.205 62	1.216 93	1.218 67	1.211 91	1.197 66	1.186 33

in the UV spectrum) forms the image of the plasma jet with a magnification of 1. A quartz optical fibre put in the focal plane of the lens is used to sample plasma radiation along a diameter of the plasma column.

We have checked that the intensity ratio of two atomic lines of Cu_I did not change along different cords of the plasma column. This observation means that the temperature profile is rather flat along a diameter of the recombining plasma column. The apparatus function of the optical device has been measured using a spectral mercury lamp. The shape of a line has been successfully fitted with a Gaussian profile and leads to a full width at 1/e of the maximum of 0.2 nm. Let us emphasize that the resolution of the optical system is too low to observe a separation of the rotational lines of the UV OH spectrum. The spectroscopic investigation is made in the near UV, in the range 290–330 nm.

4.2.2. Results and data processing. An efficient method to observe the OH spectrum in a plasma jet consists of introducing a small percentage of water vapour into the plasma [3]. A first attempt has been made by bubbling the working gas (pure argon) in through water at the input of the device. From our observations, it was very difficult to control the fraction of water injected into the plasma torch. At least, the effect of water vapour condensation on the cooled parts of the torch produced important instabilities of the plasma jet with a typical time of about 10 s.

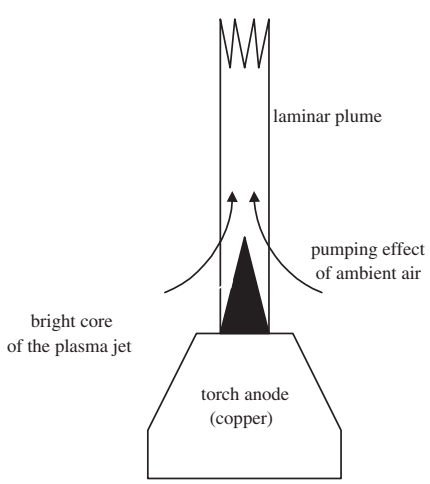

Figure 4. Pump effect of the laminar flow in ambient air.

Table 5. Maximum amplitude of the unresolved group of rotational lines G_1 as a function of the temperature and for Δ varying from 0.22–0.38 nm.

T (K)	0.22 nm	0.24 nm	0.26 nm	0.28 nm	0.30 nm	0.32 nm	0.34 nm	0.36 nm	0.38 nm
600	0.182 75	0.189 74	0.196 61	0.203 43	0.210 27	0.217 04	0.225 00	0.231 46	0.237 71
800	0.236 80	0.244 05	0.250 96	0.257 73	0.264 40	0.270 96	0.278 65	0.284 89	0.290 93
1000	0.295 13	0.302 12	0.308 61	0.314 83	0.320 83	0.326 69	0.333 54	0.339 14	0.344 60
1200	0.355 80	0.362 33	0.368 18	0.373 61	0.378 71	0.383 64	0.389 44	0.394 20	0.398 94
1400	0.416 58	0.422 72	0.427 86	0.432 44	0.436 58	0.440 54	0.445 14	0.449 03	0.452 99
1600	0.476 24	0.481 82	0.486 23	0.489 97	0.493 17	0.496 10	0.499 58	0.502 57	0.505 78
1800	0.533 56	0.538 62	0.542 37	0.545 26	0.547 57	0.549 51	0.551 84	0.554 01	0.556 53
2000	0.587 91	0.592 45	0.595 64	0.597 74	0.599 16	0.600 21	0.601 47	0.602 84	0.604 65
2200	0.638 88	0.642 98	0.645 66	0.647 06	0.647 64	0.647 84	0.648 10	0.648 73	0.649 91
2400	0.686 37	0.690 07	0.692 27	0.693 04	0.692 86	0.692 27	0.691 60	0.691 55	0.692 09
2600	0.730 39	0.733 73	0.735 48	0.735 67	0.734 81	0.733 49	0.731 98	0.731 25	0.731 25
2800	0.771 03	0.774 04	0.775 36	0.775 02	0.773 55	0.771 57	0.769 29	0.767 94	0.767 42
3000	0.808 45	0.811 12	0.812 04	0.811 22	0.809 21	0.806 63	0.803 61	0.801 74	0.800 72
3200	0.842 82	0.845 16	0.845 71	0.844 44	0.841 95	0.838 84	0.835 15	0.832 79	0.831 32
3400	0.874 36	0.876 32	0.876 53	0.874 87	0.871 95	0.868 36	0.864 09	0.861 27	0.859 39
3600	0.903 26	0.904 83	0.904 72	0.902 72	0.899 42	0.895 40	0.890 59	0.887 37	0.885 11
3800	0.929 74	0.930 90	0.930 49	0.928 17	0.924 53	0.920 12	0.914 85	0.911 26	0.908 66
4000	0.953 98	0.954 75	0.954 04	0.951 45	0.947 49	0.942 73	0.937 05	0.933 13	0.930 23
4200	0.976 16	0.976 55	0.975 56	0.972 72	0.968 47	0.963 40	0.957 35	0.953 14	0.949 97
4400	0.996 47	0.996 49	0.995 22	0.992 15	0.987 64	0.982 30	0.975 93	0.971 46	0.968 04
4600	1.015 09	1.014 73	1.013 19	1.009 92	1.005 16	0.999 59	0.992 93	0.988 23	0.984 59
4800	1.032 16	1.031 42	1.029 62	1.026 16	1.021 19	1.015 41	1.008 49	1.003 58	0.999 75
5000	1.047 83	1.046 70	1.044 65	1.041 01	1.035 85	1.029 89	1.022 74	1.017 65	1.013 64
5200	1.062 22	1.060 71	1.058 41	1.054 60	1.049 28	1.043 15	1.035 80	1.030 55	1.026 38
5400	1.075 44	1.073 55	1.071 01	1.067 04	1.061 57	1.055 31	1.047 78	1.042 39	1.038 07
5600	1.087 61	1.085 33	1.082 56	1.078 44	1.072 84	1.066 45	1.058 78	1.053 26	1.048 81
5800	1.098 81	1.096 16	1.093 16	1.088 89	1.083 18	1.076 68	1.068 88	1.063 24	1.058 69
6000	1.109 14	1.106 11	1.102 88	1.098 49	1.092 67	1.086 07	1.078 17	1.072 43	1.067 77
6200	1.118 66	1.115 28	1.111 82	1.107 30	1.101 40	1.094 71	1.086 71	1.080 89	1.076 14
6400	1.127 45	1.123 71	1.120 04	1.115 40	1.109 42	1.102 66	1.094 58	1.088 68	1.083 84
6600	1.135 58	1.131 49	1.127 60	1.122 85	1.116 80	1.109 98	1.101 83	1.095 86	1.090 96
6800	1.143 10	1.138 67	1.134 57	1.129 72	1.123 60	1.116 72	1.108 52	1.102 49	1.097 52
7000	1.150 06	1.145 29	1.140 99	1.136 04	1.129 87	1.122 94	1.114 69	1.108 62	1.103 59
7200	1.156 50	1.151 42	1.146 92	1.141 88	1.135 65	1.128 68	1.120 40	1.114 28	1.109 20
7400	1.162 46	1.157 08	1.152 39	1.147 26	1.140 99	1.133 99	1.125 68	1.119 52	1.114 39
7600	1.168 00	1.162 32	1.157 44	1.152 23	1.145 92	1.138 89	1.130 56	1.124 37	1.119 20
7800	1.173 14	1.167 17	1.162 12	1.156 83	1.150 48	1.143 43	1.135 08	1.128 87	1.123 66
8000	1.177 91	1.171 67	1.166 44	1.161 08	1.154 71	1.147 64	1.139 28	1.133 04	1.127 80

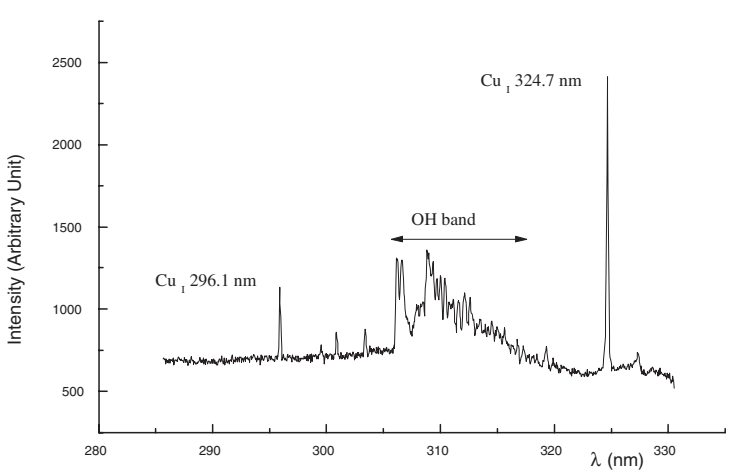

Figure 5. Spectrum recorded in the recombining plume of the laminar plasma jet. One can notice the presence of Cu_I atomic lines and the UV OH band at 306.357 nm.

Since the laminar plasma jet acts as a pump (figure 4) for the ambient air [6], we found that it was possible to observe the UV OH band at 306.357 nm without seeding the working gas with water vapour, because of the small amount of water vapour present in ambient air.

A typical recorded spectrum is given in figure 5, and exhibits both the presence of neutral copper lines, and of the UV OH band at 306.357 nm. The copper lines come from the anode that is easily eroded when the plasma jet is laminar.

The determination of the temperature can be performed

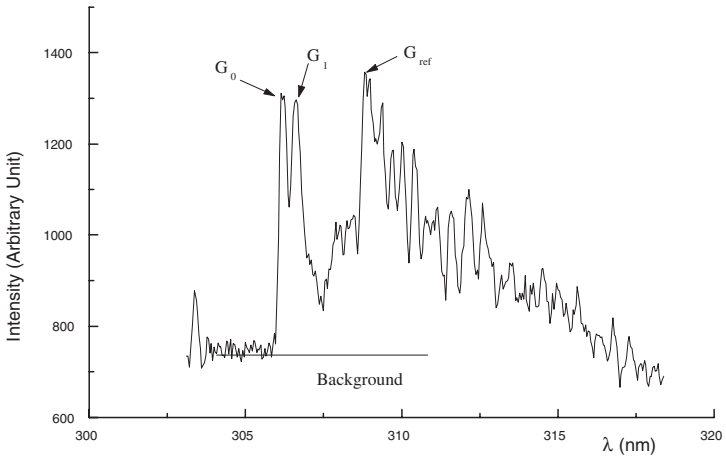

Figure 6. UV OH molecular band recorded in the plume of an argon plasma jet in ambient air.

Table 6. Atomic parameters of the copper lines observed in the plasma jet.

Wavelength λ (nm)	Energy of the upper level (cm^{-1})	Statistical weight g_u	Transition probability A (10^8 s^{-1})
296.12	44 963	8	0.0376
324.75	30 784	4	1.39

using the intensity ratio of the two main Cu_I lines available in the spectrum. The parameters of these two lines are summarized in table 6 [8].

The intensity ratio of the two lines can be expressed as a function of the temperature T under the assumption of local thermodynamic equilibrium. Using the subscripts '1' and '2' for the two lines, we have:

$$T = \frac{E_2 - E_1}{k} \ln\left(\frac{I_1 \nu_1 g_2 A_2}{I_2 \nu_2 g_1 A_1}\right)$$

where I_1 and I_2 represent the intensities, ν_1 and ν_2 the frequencies of the two lines, and k is the Boltzmann constant. The application of the intensity ratio gives the temperature $T = 4400$ K.

Figure 6 gives a plot of the UV OH band observed in the recorded spectral area. The three groups of unresolved rotational lines, labelled G_0, G_1 and G_{ref}, are easily identified (see figure 2). We have to emphasize the presence of a Cu_I line located at the wavelength $\lambda = 306.341$ nm that may give a perturbation in the intensity of the group of lines G_0. For this reason, the group of lines G_0 will not be used to carry out a temperature value.

From the measured intensity ratio of the two groups of lines, we obtain a rotational temperature of 3800 K, that is lower than the excitation temperature obtained from the intensity ratio of the copper lines. However, the rotational temperature determined by the OH spectrum calibration is very close to the temperature obtained with interferometry [7], that is an enthalpic temperature obtained using Gladstone's law.

5. Conclusion

In this paper, we have presented a very sensitive variation of a group of unresolved lines in the UV OH spectrum, that have been calibrated using numerical simulations. Calibration data are given in table form for practical use. It is clear that the main errors in a rotational temperature determination come from:

- the determination of the underlying background continuum, necessary to measure the maximum amplitudes of the groups of unresolved rotational lines;
- the evaluation of the apparatus function.

A possible direct application of this work is the elaboration of an 'OH molecular pyrometer', actually studied in our research group. A paper presenting and giving the computer program used to produce the synthetic spectra is presently in preparation.

References

[1] Gaydon A G 1957 *The Spectroscopy of Flames* (London: Chapman and Hall)
[2] Pellerin S, Koulidiati J, Motret O, Musiol K, De Graaf M, Pokrzwka B and Chapelle J 1997 *High Temp. Mater. Process.* **1** 493–509
[3] Pellerin S, Cormier J M, Richard F, Musiol K and Chapelle J 1996 *J. Phys. D: Appl. Phys.* **29** 726–39
[4] Diecke G H and Crosswhite H M 1961 *J. Quant. Spectrosc. Radiat. Transfer* **2** 97
[5] de Izarra C, Vallée O and Chapelle J 1993 *High Temp. Chem. Process.* **2** 107–13
[6] Czernichowski A 1970 *Acta Phys. Pol.* A **40** 283–94
[7] Ranson P, Vallée O and Chapelle J 1977 *Revue Phys. Appl.* **12** 1187
[8] Reader J, Corliss C H, Wiese W L and Martin G A 1980 *Wavelengths and Transition Probabilities for Atoms and Atomic Ions* (Washington, DC: National Bureau of Standards)